Seventh International Conference on CFD in the Minerals and Process Industries
CSIRO, Melbourne, Australia
9-11 December 2009

NUMERICAL SIMULATION OF HEAT TRANSFER OF NANOFLUIDS IN AN ENCLOSURE

Sapna SHARMA[1*], **Arvind Kumar GUPTA**[2]

[1,2]Mathematics Group
Birla Institute of Technology & Science Pilani
Pilani, Rajasthan, India – 333031
*Corresponding Author, E-mail: sapna2002@gmail.com

ABSTRACT

In this paper, the heat transfer and fluid flow due to buoyancy force in a square enclosure using nanofluids are studied. Four different types of model from the literature are considered for the effective viscosity of the nanofluid. Finite Element method has been applied to incorporate a homogeneous solid-liquid mixture formulation for the two-dimensional buoyancy-driven convection in the enclosure filled with three different types of nanofluids .Simulations have been carried out to investigate the effects of the volume fraction, Nusselt number and Grashof number. An increase in Nusselt number was found with the volume fraction of nanoparticles for the whole range of Grashof number. Other than the thermal conductivity, the effective dynamic viscosity found to play a major role in heat transfer enhancement as the significant difference is observed from different adopted models.

Keywords: Nanofluids; Natural convection; Finite Element Method; Enclosure

NOMENCLATURE

A Aspect ratio
c_p Specific Heat
d_p Nano particle diameter
Gr Grashof Number
H Cavity Height
L Cavity Length
k_f Fluid thermal conductivity
k_s Solid thermal conductivity
Nu Local Nusselt number
$\Pr$ Prandtlnumber
Q Total heat transfer from the left wall
U,V Dimensionalness Interistital velocity component
u,v Interistital velocity component
x,y Cartesian coordinates
X,Y Dimensionless coordinates
T Temperature

Greek symbols

α Thermal diffusivity
β_f Fluid thermal expansion coefficient
β_s Solid expansion coefficient
ϕ Solid volume fraction
ν_f Kinematic viscosity
θ Dimensionless temperature,
ω Vorticity
Ω Dimensionless vorticity
ψ' Stream function
ψ Dimensionless stream function
ρ Density
μ Dynamic viscosity

Subscripts

eff Effective
f Fluid
H Hot
L Cold
nf Nanofluid
o Reference value
s Solid

INTRODUCTION

Heat transfer fluids provide an environment for adding or removing energy to systems and their efficiencies depends on their physical properties such as thermal conductivity, viscosity, density and heat capacity. Low thermal conductivity is often the primary limitation for heat transfer fluids such as water, oil, ethylene glycol mixture in enhancing the performance and the compactness of many engineering electronic devices. To overcome this drawback there is a strong motivation to develop advanced heat transfer fluids with substantially higher conductivities to enhance thermal characteristics, suspension of colloidal particles dubbed as nanofluids. Choi (1995) in his pioneered work uses small amount of particles which are dispersed into water and other fluids. It has since then been shown experimentally by many scientists and engineers. Lee et al. (1999), Xuan et al. (2000) and Eastman et al. (2001) used nanoparticles as Oxide, Copper and Alumina particles respectively and conclude that nanofluids can have anomalously higher thermal conductivities than that of the base fluid, thus posing as a promising alternative for thermal applications.

In the literature little work has been done on natural convection phenomena in nanofluids with differentially heated enclosures. Hwang et al. (2007) investigated the buoyancy-driven heat transfer of water-based Al_2O_3 nanofluids in a rectangular cavity. They showed that the ratio of heat transfer coefficient of nanofluids to that of base fluid is decreased as the size of nanoparticles increases, or the average temperature of nanofluids is decreased. Khanafer et al. (2003) was the first to investigate the problem of buoyancy driven heat transfer enhancement of nanofluids in a two-dimensional enclosure. They tested different models for nanofluid density, viscosity, and thermal expansion coefficients and found that the suspended nanoparticles substantially increase the heat transfer rate any given Grashof number. Jou and Tzeng (2006) used the Khanafer's model and found volume fraction of nanofluids cause an increase in the average heat transfer coefficient. Jang and Choi (2004) investigated the Benard regime in nanofluid filled rectangular enclosure. Wang et al. (2006) conducted a study on natural convection in nanofluid filled vertical and horizontal enclosures Polidori et al. (2007) analyzed the heat transfer enhancement in natural convection using nanofluids. Oztop et al. (2008) analyzed numerically the natural convection in partially heated enclosures filled with nanofluids.

The aim of the present article is to study the natural convection of nanofluid in a two dimensional enclosure. In the next section, we present the mathematical formulation of the problem. In Section 3, we discussed the finite element method. Section 4 contained the result and discussion. Finally in Section 5, we provide a conclusion on results obtained.

MATHEMATICAL FORMULATION:

The geometry under consideration is a horizontal enclosure of height H and length L. It is assumed that the third dimension of the cavity is large enough so that the fluid flow and heat transfer can be considered two dimensions. The vertical walls of the enclosure are subjected to temperature T_H and T_L at the vertical left and right walls, respectively while the adiabatic boundary conditions are applied at upper and horizontal walls. The fluid in the enclosure is a water based nanofluid containing different type of nanoparticles: Cu, Al_2O_3, and TiO_2. The nanofluid is assumed incompressible and the flow is assumed to be laminar. It is assumed that the base fluid (i.e. water) and the nanoparticles are in thermal equilibrium and no slip occurs between them. The thermophysical properties of the nanofluid are given in Table 1.

The governing equations for the present study in terms of the stream function-vorticity formulation are of the following form:

Kinematics Equation
$$\frac{\partial^2\psi'}{\partial x^2}+\frac{\partial^2\psi'}{\partial y^2}=-\omega \qquad (1)$$

Energy Equation
$$u\frac{\partial T}{\partial x}+v\frac{\partial T}{\partial y}=\frac{\partial}{\partial x}\left[\left(\alpha_{nf}+\frac{k_d}{\left(\rho c_p\right)_{nf}}\right)\frac{\partial T}{\partial x}\right]+\frac{\partial}{\partial y}\left[\left(\alpha_{nf}+\frac{k_d}{\left(\rho c_p\right)_{nf}}\right)\frac{\partial T}{\partial y}\right] \qquad (2)$$

Vorticity Equation
$$u\frac{\partial\omega}{\partial x}+v\frac{\partial\omega}{\partial y}=\frac{\mu_{eff}}{\rho_{nf,o}}\nabla^2\omega+\frac{1}{\rho_{nf,o}}\left[\phi\rho_{s,o}\beta_s+(1-\phi)\rho_{f,o}\beta_f\right]g\frac{\partial T}{\partial x}, \qquad (3)$$

where $\alpha_{nf}=\dfrac{\left(k_{eff}\right)_{stagnant}}{\left(\rho c_p\right)_{nf}}$.

The effective density of a fluid containing suspended particles at a reference temperature is given by
$$\rho_{nf,o}=(1-\phi)\rho_{f,o}+\phi\rho_{s,o}. \qquad (4)$$

The effective viscosity of a fluid of viscosity μ_f containing a dilute suspension of small rigid spherical particles is given by four models.

Einstein's model (1956)
$$\mu_{eff}=\mu_f(1+2.5\phi),\quad \text{for } \phi<0.05. \qquad (5a)$$

Brinkmann (1952) as
$$\mu_{eff}=\frac{\mu_f}{(1-\phi)^{2.5}}. \qquad (5b)$$

Brownian motion effect's model (2005)
$$\mu_{eff}=\mu_f(1+2.5\phi+6.17\phi^2). \qquad (5c)$$

Pak and Cho's Correlation (1998)
$$\mu_{eff}=\mu_f(1+39.11\phi+533.9\phi^2). \qquad (5d)$$

The heat capacitance of the nanofluid can be presented as
$$(\rho c_p)_{nf}=(1-\phi)\left(\rho c_p\right)_f+\phi\left(\rho c_p\right)_s. \qquad (6)$$

The effective stagnant thermal conductivity of the solid liquid mixture was introduced by Wasp as follows
$$\frac{\left(k_{eff}\right)_{stagnant}}{k_f}=\frac{k_s+2k_f-2\phi(k_f-k_s)}{k_s+2k_f+\phi(k_f-k_s)}. \qquad (7)$$

$$k_{eff}=\left(k_{eff}\right)_{stagnant}+k_d. \qquad (8)$$

$$k_d=C\left(\rho c_p\right)_{nf}|\overline{V_1}|\phi d_p. \qquad (9)$$

where $|\overline{V_1}|=\sqrt{u^2+v^2}$ and C is an unknown constant and the value can be calculated by the experiment. Here $C=0$ corresponds to zero thermal dispersion.

The equation (1) to (3) can be cast in non-dimensional form by incorporating the following dimensionless parameters
$$X=\frac{x}{H},\qquad Y=\frac{y}{H},\qquad U=\frac{uH}{\sqrt{g\beta_T\Delta TH^3}},$$
$$V=\frac{vH}{\sqrt{g\beta_T\Delta TH^3}},\quad \Omega=\frac{\omega H^2}{\sqrt{g\beta_T\Delta TH^3}},$$
$$\psi=\frac{\psi'}{\sqrt{g\beta_T\Delta TH^3}},\quad \theta=\frac{T-T_L}{T_H-T_L}. \qquad (10)$$

$$U=\frac{\partial\psi}{\partial Y},\qquad V=-\frac{\partial\psi}{\partial X}. \qquad (11)$$

$$\frac{\partial^2\psi}{\partial X^2}+\frac{\partial^2\psi}{\partial Y^2}=-\Omega. \qquad (12)$$

$$U\frac{\partial\Omega}{\partial X}+V\frac{\partial\Omega}{\partial Y}=\frac{\nabla^2\Omega}{\left(1-\phi\right)^{2.5}\left[\phi\dfrac{\rho_{s,o}}{\rho_{f,o}}+\left(1-\phi\right)\right]\sqrt{Gr}}+\lambda\frac{\partial\theta}{\partial X}. \qquad (13)$$

$$U\frac{\partial\theta}{\partial X}+V\frac{\partial\theta}{\partial Y}=\frac{1}{\Pr\sqrt{Gr}}\left[\frac{\partial}{\partial X}\left(\chi\frac{\partial\theta}{\partial X}\right)+\frac{\partial}{\partial Y}\left(\chi\frac{\partial\theta}{\partial Y}\right)\right]. \quad (14)$$

$$\chi=\frac{\left[\dfrac{\left(k_{eff}\right)_{stagnant}}{k_f}\right]}{(1-\phi)+\phi\dfrac{\left(\rho c_p\right)_s}{\left(\rho c_p\right)_f}}+C\phi\frac{d_p}{H}\Pr\sqrt{Gr}\sqrt{U^2+V^2} \quad (15)$$

where $Gr=\dfrac{g\beta_f\Delta TH^3}{\nu_f^2}$, $\Pr=\dfrac{\nu_f}{\alpha_f}$, and $A=\dfrac{L}{H}$ which is assumed unity in the investigation. The diameter of the nanoparticle d_p is taken as 10 nm in the present study. The physical dimension of the enclosure H is chosen to be 1 cm. The coefficient λ that appears next to the buoyancy term is given as

$$\lambda=\left[\frac{\beta_s}{1+\dfrac{(1-\phi)}{\phi}\dfrac{\rho_{f,o}}{\rho_{s,o}}\beta_f}+\frac{1}{1+\dfrac{\phi}{(1-\phi)}\dfrac{\rho_{s,o}}{\rho_{f,o}}}\right]=\frac{\beta_{nf}}{\beta_f}. \quad (16)$$

The Boundary conditions are as follows:

$$U=V=\psi=\frac{\partial\theta}{\partial Y}=0,\quad \Omega=-\frac{\partial^2\psi}{\partial Y^2},\quad \text{at } Y=0,1 \text{ and } 0\le X\le 1 \quad (17)$$

$$U=V=\psi=0,\quad \theta=0.5,\quad \Omega=-\frac{\partial^2\psi}{\partial X^2},\quad \text{at } X=0,\ 0\le Y\le 1 \quad (18)$$

$$U=V=\psi=0,\quad \theta=-0.5,\quad \Omega=-\frac{\partial^2\psi}{\partial X^2},\quad \text{at } X=1,\ 0\le Y\le 1 \quad (19)$$

Lots of factor such as thermal conductivity, heat capacitance of both the pure fluid and ultrafine particles, the volume fraction of the suspended particles, the dimension of these particles, flow structure and the viscosity are effecting the Nusselt number of nanofluid. The local variation of the Nusselt number are given by

$$Nu=\frac{Q}{Q_{cond,fluid}}=-\frac{k_{eff}}{k_f}\frac{\partial\theta}{\partial X}, \quad (20)$$

where $Q=-\left(k_{eff}\right)_{stagnant}A\dfrac{\partial T}{\partial x}\Big|_{x=0}$. (21)

Physical Properties	Fluid phase (water)	Cu	Al_2O_3	TiO_3
C_p(J/kgK)	4179	385	765	686.2
$\rho(kg/m^3)$	997.1	8933	3970	4250
k(W/mK)	0.613	400	40.0	8.9538
$\alpha\times10^7(m^2/s)$	1.47	1163.1	131.7	30.7
$\beta\times10^{-5}(1/K)$	21.0	1.67	0.85	0.9

Table 1: Thermophysical properties of fluid and Nanoparticles

NUMERICAL METHOD

The finite element method has been used to solve the nonlinear system of equations (11) to (14).

Variational Formulation

The variational form associated with equations (11) to (14) over a typical square element is given by**:**

$$\int_{Y_e}^{Y_{e+1}}\int_{X_e}^{X_{e+1}} w_1\left(U-\frac{\partial\psi}{\partial Y}\right)dX\,dY=0. \quad (22)$$

$$\int_{Y_e}^{Y_{e+1}}\int_{X_e}^{X_{e+1}} w_2\left(V+\frac{\partial\psi}{\partial X}\right)dX\,dY=0. \quad (23)$$

$$\int_{Y_e}^{Y_{e+1}}\int_{X_e}^{X_{e+1}} w_3\left(\frac{\partial^2\psi}{\partial X^2}+\frac{\partial^2\psi}{\partial Y^2}+\Omega\right)dX\,dY=0. \quad (24)$$

$$\int_{Y_e}^{Y_{e+1}}\int_{X_e}^{X_{e+1}} w_4\left(U\frac{\partial\Omega}{\partial X}+V\frac{\partial\Omega}{\partial Y}-\frac{\nabla^2\Omega}{(1-\phi)^{2.5}\left[\phi\dfrac{\rho_{s,o}}{\rho_{f,o}}+(1-\phi)\right]\sqrt{Gr}}-\lambda\frac{\partial\theta}{\partial X}\right)dX\,dY=0 \quad (25)$$

$$\int_{Y_e}^{Y_{e+1}}\int_{X_e}^{X_{e+1}} w_5\left(U\frac{\partial\theta}{\partial X}+V\frac{\partial\theta}{\partial Y}-\frac{1}{\Pr\sqrt{Gr}}\left[\frac{\partial}{\partial X}\left(\chi\frac{\partial\theta}{\partial X}\right)+\frac{\partial}{\partial Y}\left(\chi\frac{\partial\theta}{\partial Y}\right)\right]\right)dX\,dY=0. \quad (26)$$

where w_1, w_2, w_3, w_4 and w_5 are arbitrary test function. All functions satisfy the homogeneous boundary conditions, as per theoretical requirements.

Finite Element Formulation

The structure domain defined as: $0\le X\le 1$ and $0\le Y\le 1$ is discretized into square elements of same size. The finite element model, obtained from equations (22-26), by substituting finite element approximations of the form**.**

$$U=\sum_{j=1}^{4}U_j\xi_j,\quad V=\sum_{j=1}^{4}V_j\xi_j,\quad \psi=\sum_{j=1}^{4}\psi_j\xi_j, \quad (27)$$

$$\theta=\sum_{j=1}^{4}\theta_j\xi_j,\quad \Omega=\sum_{j=1}^{4}\Omega_j\xi_j.$$

with $w_i=\xi_j \qquad (i=1,2,3,4,5,\ j=1,2,3,4)$

where ξ_1,ξ_2,ξ_3 and ξ_4 are the linear interpolation functions for a rectangular element Ω^e and have been taken as:

$$\xi_1=\frac{(x_{e+1}-x)}{(x_{e+1}-x_e)}\frac{(y_{e+1}-y)}{(y_{e+1}-y_e)},\quad \xi_2=\frac{(x-x_e)}{(x_{e+1}-x_e)}\frac{(y_{e+1}-y)}{(y_{e+1}-y_e)}, \quad (28)$$

$$\xi_3=\frac{(x-x_e)}{(x_{e+1}-x_e)}\frac{(y-y_e)}{(y_{e+1}-y_e)},\quad \xi_4=\frac{(x_{e+1}-x)}{(x_{e+1}-x_e)}\frac{(y-y_e)}{(y_{e+1}-y_e)}.$$

The finite element model of the equations thus formed is given by

$$\begin{bmatrix} [K^{11}] & [K^{12}] & [K^{13}] & [K^{14}] & [K^{15}] \\ [K^{21}] & [K^{22}] & [K^{23}] & [K^{24}] & [K^{25}] \\ [K^{31}] & [K^{32}] & [K^{33}] & [K^{34}] & [K^{35}] \\ [K^{41}] & [K^{42}] & [K^{43}] & [K^{44}] & [K^{45}] \\ [K^{51}] & [K^{52}] & [K^{53}] & [K^{54}] & [K^{55}] \end{bmatrix} \begin{bmatrix} \{U\} \\ \{V\} \\ \{\psi\} \\ \{\Omega\} \\ \{\theta\} \end{bmatrix} = \begin{bmatrix} \{b^1\} \\ \{b^2\} \\ \{b^3\} \\ \{b^4\} \\ \{b^5\} \end{bmatrix} \quad (29)$$

where $[K^{mn}]$ and $[b^m]$ $(m, n = 1,2,3,4,5)$ are defined as:

$$K_{ij}^{11} = \int_{\Omega^e} \xi_i \xi_j dXdY, \quad K_{ij}^{13} = \int_{\Omega^e} \xi_i \frac{\partial \xi_j}{dY} dX\,dY, \; K_{ij}^{12} = K_{ij}^{14} = K_{ij}^{15} = 0. \quad (30)$$

$$K_{ij}^{22} = \int_{\Omega^e} \xi_i \xi_j dXdY, K_{ij}^{23} = -\int_{\Omega^e} \xi_i \frac{\partial \xi_j}{dX} dX\,dY, K_{ij}^{21} = K_{ij}^{24} = K_{ij}^{25} = 0. \quad (31)$$

$$K_{ij}^{33} = -\int_{\Omega^e} \left(\frac{\partial \xi_i}{dX} \frac{\partial \xi_j}{dX} + \frac{\partial \xi_i}{dY} \frac{\partial \xi_j}{dY} \right) dXdY, K_{ij}^{34} = \int_{\Omega^e} \xi_i \xi_j dX\,dY, K_{ij}^{31} = K_{ij}^{32} = K_{ij}^{35} = 0. \quad (32)$$

$$K_{ij}^{44} = \int_{\Omega^e} \left(\overline{U} \xi_i \frac{\partial \xi_j}{dX} + \overline{V} \xi_i \frac{\partial \xi_j}{dY} \right) dXdY + \int_{\Omega^e} \left[\frac{\left(\frac{\partial \xi_i}{dX} \frac{\partial \xi_j}{dX} + \frac{\partial \xi_i}{dY} \frac{\partial \xi_j}{dY} \right)}{(1-\phi)^{2.5} \left\{ \phi \frac{\rho_{s,o}}{\rho_{f,o}} + (1-\phi) \right\} \sqrt{Gr}} \right] dXdY. \quad (33)$$

$$K_{ij}^{45} = -\lambda \int_{\Omega^e} \xi_i \frac{\partial \xi_j}{dX} dX\,dY, K_{ij}^{41} = K_{ij}^{42} = K_{ij}^{43} = 0,$$

$$K_{ij}^{55} = \int_{\Omega^e} \left(\overline{U} \xi_i \frac{\partial \xi_j}{dX} + \overline{V} \xi_i \frac{\partial \xi_j}{dY} \right) dXdY + \int_{\Omega^e} \left\{ \frac{\left(\frac{\partial \xi_i}{dX} \frac{\partial \xi_j}{dX} \overline{\chi} + \frac{\partial \xi_i}{dY} \frac{\partial \xi_j}{dY} \overline{\chi} \right)}{\Pr \sqrt{Gr}} \right\} dXdY. \quad (34)$$

$$K_{ij}^{51} = K_{ij}^{52} = K_{ij}^{53} = K_{ij}^{54} = 0. \quad (35)$$

$$b_i^1 = 0, \quad b_i^2 = 0, \quad b_i^3 = \oint_{\Gamma^e} \xi_i q_{n_3} ds,$$
$$b_i^4 = \oint_{\Gamma^e} \xi_i q_{n_4} ds, \quad b_i^5 = \oint_{\Gamma^e} \xi_i q_{n_5} ds, \quad (36)$$

where $\overline{U} = \sum_{i=1}^{4} \xi_i U_i, \quad \overline{V} = \sum_{i=1}^{4} \xi_i V_i$,

$$q_{n_2} = -\left(n_X \frac{\partial \psi}{\partial X} + n_Y \frac{\partial \psi}{\partial Y} \right),$$

and

$$q_{n_4} = \left(n_X \frac{\partial \Omega}{\partial X} + n_Y \frac{\partial \Omega}{\partial Y} \right), \quad (37)$$

$$q_{n_5} = \left(n_X \overline{\chi} \frac{\partial \theta}{\partial X} + n_Y \overline{\chi} \frac{\partial \theta}{\partial Y} \right)$$

The whole domain is divided into square elements. Each element is four nodded. At each node five functions are to be evaluated hence after assembly of the element equations, we obtain a system of equations which is nonlinear therefore an iterative scheme is used to solve it. The system is linearized by incorporating the functions $\overline{U}$ and $\overline{V}$, which are assumed to be known. The system of linear equations has been solved by using Gauss elimination method by maintaining an accuracy of four significant digits.

RESULTS AND DISCUSSIONS

The finite element method has been used to solve the nonlinear system of equations (11) to (14).The controlling parameter that define the fluid flow, heat and natural convection in an enclosure are aspect ratio A, Gr, ϕ and $\Pr$. It needs quite extensive analysis to cover effects of each parameter. It is intended to limit the analysis for Grashof number $10^3 \le Gr \le 10^5$, $0 \le \phi \le 0.25$ as model of nanofluid and for an aspect ratio of 1 as a square enclosure. The thermophysical properties of fluid and solid phase are shown in table 1. A grid independence study is conducted using three different grid sizes of 41×41, 61×61 and 81×81 for aspect ratio of 1. It is observed that further refinement of grids from 61×61 to 81×81 do not have a significant effect on the results. Based upon these observations, a uniform grid of 61×61 points is used for all calculations of aspect ratio of 1.

Fig. 1 (a)-(d) demonstrate the typical features of the volume fraction ϕ on the stream line and isotherms for fixed value of the Grashof number. Fig.1 (a) shows the representive sequence of stream line isotherms pattern in a square domain for $\phi = 0$. In this study the flow consist of single roll, the tendency of which is to rearrange the fluid into a position of stable stratification, one in which the warm fluid that initially occupied the left half eventually moves to the upper half of the domain. Fig.1 (b) to 1 (d) indicates, as the volume fraction increases, the velocity at the centre of the enclosure increase as a result of higher solid-fluid transportation of heat. Flow strength also increases with increasing of volume fraction of nano particles.

The variation of the Nusselt number for different volume fraction of nanoparticle is shown in fig. 2. Volume fraction increases implies that more and more particles will be suspended so that thermal conductivity increased. Physically the heat transfer will also increase. It is clear from the graph that the heat transfer increases when increasing the volume fraction of nanoparticles.

The effect of Grashof number for pure fluid and nanofluids is depicted in Fig. 3. For a fixed aspect ratio, when Grashof number increases Nusselt number also increases. It is clear from the figure that the presence of the nanoparticles plays a significant role to increase the heat transfer.

Fig. 4 demonstrates the effect of particles diameter on Nusselt number. Comparison is also being done for Brinkman's model and Pak and Cho's Model for dynamic viscosity. Since four models have been taken for dynamic viscosity but the results of Einstein's model, Brinkman's model and Brownian motion effects model are similar so only the comparison of two models have been taken. As the size of the nanoparticles increases, the Nusselt number of the nanofluid decreased. The ratio of the thermal conductivity is remarkably decreased as the size of the nanoparticles increases. So the Nusselt number of the nanofluids is decreased as the diameter of the nanoparticle increases.

Fig. 5 represents the variation of the Nusselt number with volume fraction using different nanoparticles for a fix value of Grashof number. The figure shows that the heat transfer increases almost monotonically with increase in volume fraction for all nanofluids.

CONCLUSION

The major findings contained in this paper are as follows: the natural convection of water based nanofluids is more stable than base fluids in a square enclosure heated from side, as the volume fraction of nanoparticles increases the size of the nanoparticle decreases, or the average temperature of nanofluids increases. In addition, as the viscosity increases the heat transfer coefficient derived from Brinkman's model evaluating lower effective viscosity increase but the coefficient with Pak and Cho's model is decreased. The results indicate that the Nusselt number increases as the volume fraction increases. The presence of the nanoparticles in the fluid changes the characteristics of the base fluids. A comparative study of different nanofluids based on the physical properties of noparticles is analyzed and found that Cu nanoparticles have high value of thermal diffusivity.

REFERENCES

AMIRI, A. and VAFAI, K., (1994), "Analysis of dispersion effects and nonthermal equilibrium, non-Darcian, variable porosity, incompressible flow through porous media", *Int. J. Heat Mass Transfer*, **37**, 939–954.

BRINKMAN, H.C., (1952), "The viscosity of concentrated suspensions and solutions" *J. Chem. Phys.*, **20**, 571–581.

CHOI, S. U. S., (1995), "Enhancing thermal conductivity of fluids with nanoparticles", *ASME FED*, **231**, pp. 99–105.

EASTMAN, J. A., CHOI, S. U. S., LI, S., YU, W. and THOMPSON, L.J., (2001), "Anomalously increased effective thermal conductivities of ethylene glycolbased nanofluids containing copper nanoparticles" *Appl. Phys. Lett.*, **78**, 718–720.

EINSTEIN, A., (1956) "Investigation on the theory of Brownian Motion", *Dover*, New York.

HWANG, K. S., LEE, JI-HWAN and JANG, S. P., (2007) "Buoyancy-driven heat transfer of water based Al_2O_3 nanofluids in a rectangular cavity", *Int. J. Heat Mass Transfe,r* **50**, 4003–4010.

JANG, S. P. and CHOI, S. U. S., (2004) "Free convection in a rectangular cavity (Benard convection) with nanofluids", *Proceedings of IMECE*. Anaheim, California, USA.

JOU, R.Y. and TZENG, S. C., (2006), "Numerical research of nature convective heat transfer enhancement filled with nanofluids in rectangular enclosures". *Int. Comm. Heat Mass Transfer*, **33**, 727–736.

KHANAFER, K., VAFAI, K. and LIGHTSTONE, M., (2003), "Buoyancy-driven heat transfer enhancement in a two-dimensional enclosure utilizing nanofluids", *Int. J. Heat Mass Transfer*, **46**, 3639–3653.

LEE, S., CHOI, S. U. S. and EASTMAN, J. A., (1999) "Measuring thermal conductivity of fluids containing oxide nanoparticles', *J. Heat Transfer*, **121**, 280–289.

OROZCO, D., (2005), "Hydrodynamic behavior of suspension of polar particles", *Encyclopedia surface Colloidal Sci*, **4**, 2375-2396.

OZTOP, H. F. and EIYAD A. N., (2008), **"**Numerical study of natural convection in partially heated rectangular enclosures filled with nanofluids", *Int. J. Heat Fluid Flow*, **29**, 1326-1329.

PAK, B.C. and CHO, Y., (1998), "Hydrodynamic and heat transfer study of dispersed fluids with submicron metallic oxide particle", *Exp. Heat Transfer*, **11**, 151-170.

POLIDORI, G., FOHANNO S. and NGUYEN, C. T., (2007), "A note on heat transfer modeling of Newtonian nanofluids in laminar free convection", *Int. J. Therm. Sci*, **46**, 739–744.

WASP, F. J., (1977), "Solid–liquid slurry pipeline transportation". *Trans. Tech.*, Berlin.

XIE, H., WANG, J., XIE, T.G., LIU, Y. and AI, F., (2002), "Thermal conductivity enhancement of suspensions containing nanosized alumina particles" *J. Appl. Phys.*, **91**, 4568–4572.

XUAN, Y.M. and LI, Q., (2000), "Heat transfer enhancement of nanofluids", *Int. J. Heat Fluid Flow*, **21**, 58–64.

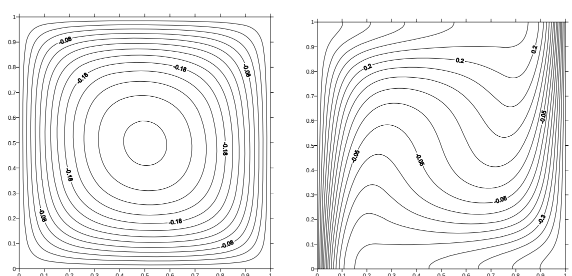

Fig. 1(a) Φ = 0.0

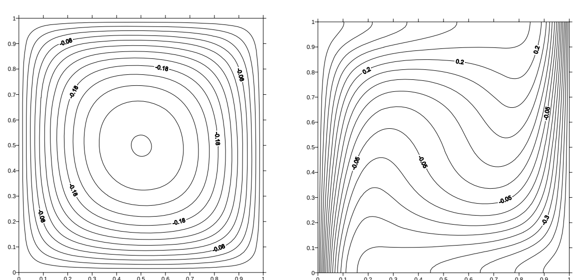

Fig. 1(a) Φ = 0.01

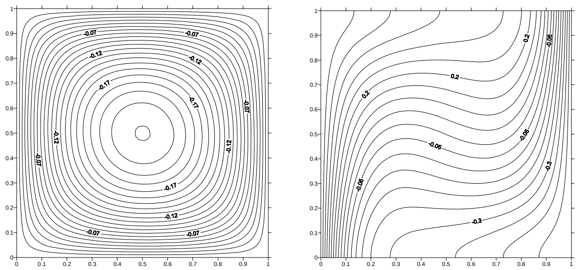

Fig. 1(a) Φ = 0.1

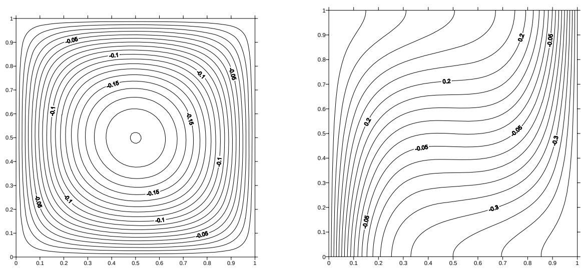

Fig. 1(a) Φ = 0.21

Fig. 1 Stream line contours & Isotherms at various fraction parameters (*Gr* = 10000, *Pr* = 0.7)

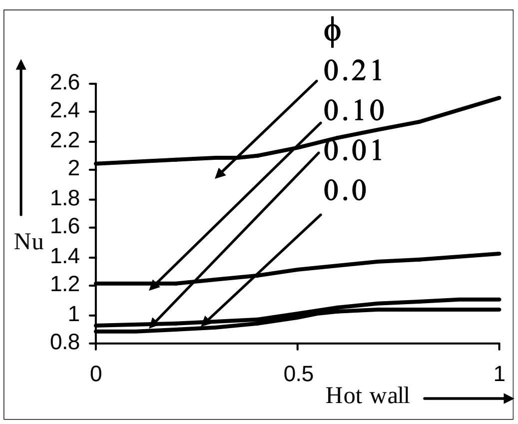

Fig. 2 Variation of the Local Nusselt number along the hot wall for different Volume fraction (*Gr* = 10000, *Pr* = 0.7)

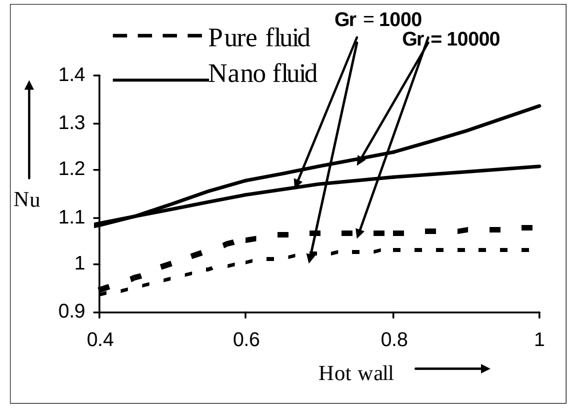

Fig. 3 Variation of the Local Nusselt number along the hot wall for different Grashoff number (Φ =.07, *Pr* = 0.7)

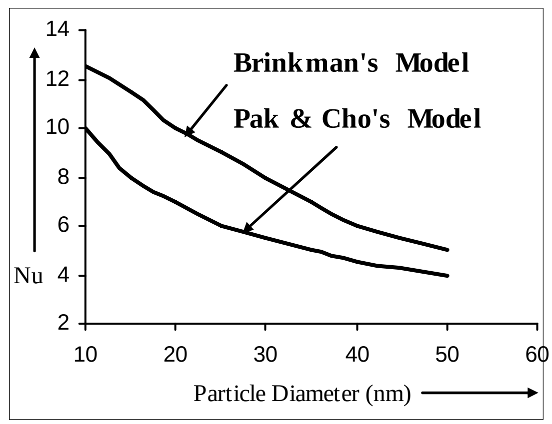

Fig. 4 Variation of the Local Nusselt number with particle diameter for diffrerent Model .(Φ =.07, *Pr* = 0.7, *Gr* = 10000)

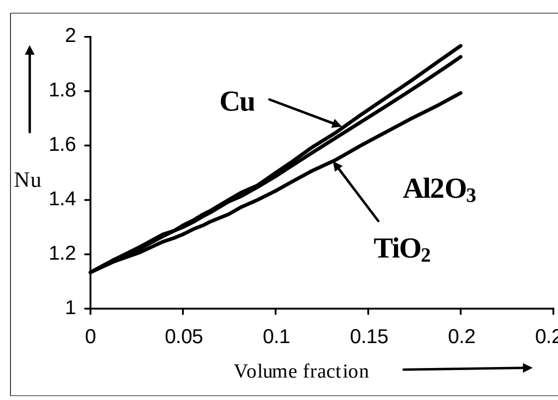

Fig. 5 Variation of the Local Nusselt number with Volumefraction for diffrerent nanofluids, (*Gr* = 10000, *Pr* = 0.7)